Advances in Concrete Construction, *Vol. 9, No. 4* (*2020*) *397-406*
DOI: https://doi.org/10.12989/acc.2020.9.4.397

Analysis of post-buckling of higher-order graphene oxide reinforced concrete plates with geometrical imperfection

Seyed Sajad Mirjavadi[1], Masoud Forsat*[1], Yahya Zakariya Yahya[2], Mohammad Reza Barati[3], Anirudh Narasimamurthy Jayasimha[4] and Imran Khan[5]

[1]*Department of Mechanical and Industrial Engineering, Qatar University, P.O. Box 2713, Doha, Qatar*
[2]*Auckland Bioengineering Institute, the University of Auckland, Auckland, New Zealand*
[3]*Fidar project Qaem Company, Darvazeh Dolat, Tehran, Iran*
[4]*Bonn-Rhein-Sieg University of Applied Science, Sankt Augustin, Germany*
[5]*Department of Electrical Engineering, University of Engineering & Technology, Peshawar 814, Pakistan*

(*Received January 27, 2020, Revised February 29, 2020, Accepted March 6, 2020*)

Abstract. The present article deals with post-buckling of geometrically imperfect concrete plates reinforced by graphene oxide powder (GOP) based on general higher order plate model. GOP distributions are considered as uniform and linear models. Utilizing a shear deformable plate model having five field components, it is feasible to verify transverse shear impacts with no inclusion of correction factor. The nonlinear governing equations have been solved via an analytical trend for deriving post-buckling load-deflection relations of the GOP-reinforced plate. Derived findings demonstrate the significance of GOP distributions, geometric imperfectness, foundation factors, material compositions and geometrical factors on post-buckling properties of reinforced concrete plates.

Keywords: post-buckling; general plate theory; concrete plate; graphene oxide powder; nonlinear stability

1. Introduction

Based on recent developments, a variety of carbon based structures containing carbon nanotube or carbon fiber have been widely utilized in composites for enhancing their mechanics and thermal specifications (Zhang 2017, Keleshtreri *et al*. 2016, Belbachir *et al*. 2019, Draoui *et al*. 2019, Medani *et al*. 2019). A 273% enhancement of elastic modulus is obtained by Ahankari *et al*. (2010) for carbon reinforced composites in comparison to conventional composites. Likewise, Gojny *et al*. (2004) mentioned that structural stiffness of carbon based composites may be enhanced with incorporation of carbon nanotube within material. Impacts of configuration and scale of carbon nanotubes on rigidity growth of material composites having metallic matrices are studied by Esawi *et al*. (2011). Because of possessing above mentioned properties, beam and plate structures having carbon based fillers are researched to understand their static or dynamical status (Yang *et al*. 2017, Semmah *et al*. 2019, Hussain *et al*. 2019). There are also some investigations on composite or functionally graded materials and interested readers are refaced to new investigations on materials (Barati and Zenkour 2018, Shafiei *et al*. 2017, Mirjavadi *et al*. 2017, 2018, 2019, Azimi *et al*. 2017, 2018, Hellal *et al*. 2019, Tlidji *et al*. 2019, Chaabane *et al*. 2019, Dehrouyeh-Semnan 2018, Dehrouyeh-Semnani *et al*. 2019, Dehrouyeh-Semnani and Jafarpour 2019, Keddari *et al*. 2020, Berghouti *et al*. 2019, Bourada *et al*. 2019, Sahla *et al*. 2019, Khiloun *et al*. 2019, Boutaleb *et al*. 2019, Boulefrakh *et al*. 2019, Boukhlif *et al*. 2019). Furthermore, the graphene based composite material has been recently gained enormous attentions because of having easy producing procedure and high rigidity growth. Nieto *et al*. (2017) presented a review paper based on several graphene based composite material possessing ceramic or metallic matrices. The multi-scale study of mechanical attributes for graphene based composite material has been provided by Lin *et al*. (2018) utilizing finite elements approach.

Until now, many of researches in the fields of nano-composites have been interested in production and materials characteristics recognition of graphene based composites and structural components containing slight percentages of graphene fillers. For instance, it is mentioned by Rafiee *et al*. (2009) that some material characteristics of graphene based composites may be enhanced via placing 0.1% volume of graphene filler. However, achieving to this level of reinforcement employing nanotubes required 1% of their volume. Graphene based composites containing epoxy matrix were created by King *et al*. (2013) by placing 6% weight fraction of graphene fillers to polymeric phases. It was stated that Young modulus of the composite has been increased from 2.72 GPa to 3.36 GPa. Next, 57% increment for Young modulus has been achieved by Fang *et al*. (2009) based on a sample of graphene based composite.

Moreover, many studies in the fields of nano-mechanic are associated with vibrational and stability investigation of various structural elements containing beam or plate reinforced via diverse graphene dispersions. For instance,

*Corresponding author, Ph.D.
E-mail: masoudforsatlar@gmail.com

Copyright © 2020 Techno-Press, Ltd.

ISSN: 2287-5301 (Print), 2287-531X (Online)

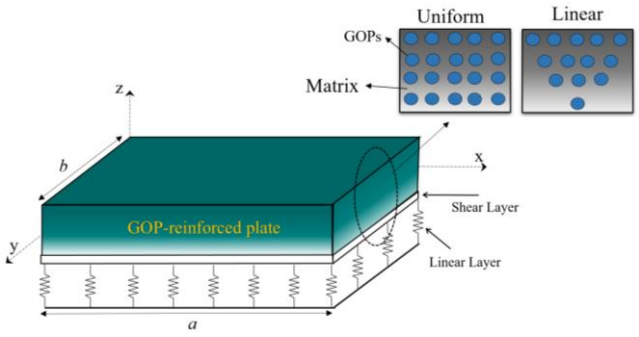

Fig. 1 Geometry of GOP-reinforced plate on elastic substrate

vibrational properties of a laminated graphene based plate have been explored by Song *et al*. (2017) assuming simply support edge condition. They assumed that the plate is constructed from particular numbers of layers each containing a sensible content of graphene. Selecting a perturbation approach, static deflections and bucking loads of graphene based plates have been derived by Shen *et al*. (2017). In above papers, each material property has discontinuous variation across the thickness of beam or plate. Also, geometrically nonlinear vibration frequencies of graphene based beams having embedded graphene have been explored by Feng *et al*. (2017) selecting first-order beam theory. Moreover, vibration frequencies of graphene based beams having porosities have been explored by Kitipornchai *et al*. (2017).

Furthermore, reinforcement of concrete with nano-size inclusions is a novel case study (Alijani and Bidgoli 2018, Guenaneche *et al*. 2019, Zaheer *et al*. 2019, Alimirzaei *et al*. 2019). Many researches show that mechanical properties of concrete can be enhanced by adding graphene platelets (GPLs), graphene oxide powders (GOPs) and ever carbon nanotubes (Du *et al*. 2016, Shamsaei *et al*. 2018). Graphene oxide, as derivative of graphene, is broadly and economically available from graphite mass oxidations. It is compatible with many matix materials including polymeric materials and even concrete (Mohammed *et al*. 2017). Graphene oxide composite exhibits great Young modulus and tensile strength as are carbon-based material with remarkable performances and low costs (Zhang *et al*. 2020). To the best of author's knowledge, post-buckling study of geometrically imperfect concrete plates reinforced by GOPs is not carried out till to now.

The present article is devoted to analyze post-buckling behaviors of a geometrically imperfect concrete plate reinforced with graphene oxide powders (GOPs) based on five-variable plate theory. GOPs have two types of dispersion within the structure including uniform-type and linear-type. The presented formulation is based upon a higher order plate accounting for shear deformations. So, it is useful for thick plates. The GOP-reinforced plate is exposed to an in-plane mechanical load (Wang and Su 2013) leading to its buckling. Via an analytical procedure, post-buckling path of the beam has been derived. It will be demonstrated that buckling characteristics of the GOP-reinforced plate are dependent on shear deformation, geometric amplitude, GOP distribution and foundation factors.

2. GOP-based composites

According to Fig. 1, it is assumed that GOPs have two types of dispersion within the structure including uniform-type and linear-type. In this figure, a GOP reinforced composite plate is illustrated. Micro-mechanic theory of such composite materials (Liew *et al*. 2015) introduces the below relationship between GOPs weight fraction (W_{GOP}) and their volume fraction (V_{GOP}) by

$$V_{GOP}^{*}=\frac{W_{GOP}}{W_{GOP}+\frac{\rho_{GOP}}{\rho_M}-\frac{\rho_{GOP}}{\rho_M}W_{GOP}} \tag{1}$$

where ρ_{GOP} and ρ_M define the mass densities of GOP and matrices, respectively. Next, the elastic modulus of a GOP based composite might be represented based upon matrix elastic modulus (E_M) by (Zhang *et al*. 2020)

$$\begin{aligned}E_1=0.49&\left(\frac{1+\xi_L^{GOP}\eta_L^{GOP}V_{GOP}}{1-\eta_L^{GOP}V_{GOP}}\right)E_M\\&+0.51\left(\frac{1+\xi_W^{GOP}\eta_W^{GOP}V_{GOP}}{1-\eta_W^{GOP}V_{GOP}}\right)E_M\end{aligned} \tag{2}$$

so that ξ_L^{GOP} and ξ_W^{GOP} define two geometrical factors indicating the impacts of graphene configuration and scales as

$$\xi_L^{GOP}=\frac{2d_{GOP}}{t_{GOP}} \tag{3a}$$

$$\eta_L^{GOP}=\frac{\left(E_{GOP}/E_M\right)-1}{\left(E_{GOP}/E_M\right)+\xi_L^{GOP}} \tag{3b}$$

$$\xi_W^{GOP}=\frac{2d_{GOP}}{t_{GOP}} \tag{3c}$$

$$\eta_W^{GOP}=\frac{\left(E_{GOP}/E_M\right)-1}{\left(E_{GOP}/E_M\right)+\xi_W^{GOP}} \tag{3d}$$

so that d_{GPL} and t_{GPL} define GOP average diameter and thickness, respectively. Furthermore, Poisson's ratio for GOP based composite might be defined based upon Poisson's ratio of the two constituents in the form

$$\nu_1=\nu_{GOP}V_{GOP}+\nu_M V_M \tag{4}$$

in which V_M=1−V_{GOP}expresses the volume fractions of matrix component (Metwally *et al*. 2014). Herein, three dispersions of the GOP have been assumed as:

Uniform

$$V_{GOP}=V_{GOP}^{*} \tag{5}$$

Linear

$$V_{GOP}=(1+2\frac{z}{h})V_{GOP}^{*} \tag{6}$$

3. Derivation of equations of motion

A general shear deformable plate theory having five field components (Barati 2017, Mouffoki *et al*. 2017, Fenjan *et al*. 2019, Ahmed *et al*. 2019, Zemri *et al*. 2015, Bounouara *et al*. 2016, Abualnour *et al*. 2019, Adda Bedia *et al*. 2019, Batou *et al*. 2019, Meksi *et al*. 2019) employs the below displacements field based on lateral (w), in-plane (u, v) and rotation (ψ_x, ψ_y) variables as (Draiche *et al*. 2019, Addou *et al*. 2019)

$$u_1(x,y,z)=u(x,y)-(z-z^*)\frac{\partial w}{\partial x}+[\Phi(z)-z^{**}]\psi_x \tag{7}$$

$$u_2(x,y,z)=v(x,y)-(z-z^*)\frac{\partial w}{\partial y}+[\Phi(z)-z^{**}]\psi_y \tag{8}$$

$$u_3(x,y,z)=w(x,y) \tag{9}$$

Thus, the shear function has been selected as (Ahmed *et al*. 2019)

$$\Phi(z)=\frac{h}{\pi}\sin\left(\frac{\pi z}{h}\right) \tag{10}$$

and

$$z^*=\frac{\int_{-h/2}^{h/2}E(z)\,z\,dz}{\int_{-h/2}^{h/2}E(z)\,dz},\quad z^{**}=\frac{\int_{-h/2}^{h/2}E(z)\,\Phi(z)\,dz}{\int_{-h/2}^{h/2}E(z)\,dz} \tag{11}$$

Therefore, the strain components may be derived as (Zarga *et al*. 2019, Zaoui *et al*. 2019, Mahmoudi *et al*. 2019)

$$\begin{Bmatrix}\varepsilon_x\\ \varepsilon_y\\ \gamma_{xy}\end{Bmatrix}=\begin{Bmatrix}\varepsilon_x^0\\ \varepsilon_y^0\\ \gamma_{xy}^0\end{Bmatrix}+z\begin{Bmatrix}k_x\\ k_y\\ k_{xy}\end{Bmatrix}+\Phi(z)\begin{Bmatrix}\chi_x\\ \chi_y\\ \chi_{xy}\end{Bmatrix},\quad \begin{Bmatrix}\gamma_{yz}\\ \gamma_{xz}\end{Bmatrix}=\Phi'(z)\begin{Bmatrix}\gamma_{yz}^0\\ \gamma_{xz}^0\end{Bmatrix} \tag{12}$$

in which

$$\begin{gathered}\varepsilon_x^0=\frac{\partial u}{\partial x}+\frac{1}{2}\left(\frac{\partial w}{\partial x}\right)^2,\ \varepsilon_y^0=\frac{\partial v}{\partial y}+\frac{1}{2}\left(\frac{\partial w}{\partial y}\right)^2,\\ \gamma_{xy}^0=\frac{\partial u}{\partial y}+\frac{\partial v}{\partial x}+\frac{\partial w}{\partial x}\frac{\partial w}{\partial y},\\ k_x=-\frac{\partial^2 w}{\partial x^2},\ k_y=-\frac{\partial^2 w}{\partial y^2},\ k_{xy}=-2\frac{\partial^2 w}{\partial x\partial y},\\ \chi_x=\psi_{x,x},\ \chi_y=\psi_{y,y},\ \chi_{xy}=\psi_{x,y}+\psi_{y,x},\\ \gamma_{yz}^0=\psi_y,\ \gamma_{xz}^0=\psi_x\end{gathered} \tag{13}$$

Also, the constitutive relations based on five-unknown plate theory may be expressed by (Faleh *et al*. 2018, She *et al*. 2018)

$$\begin{Bmatrix}\sigma_x\\ \sigma_y\\ \sigma_{xy}\\ \sigma_{yz}\\ \sigma_{xz}\end{Bmatrix}=\frac{E(z)}{1-\nu^2}\begin{pmatrix}1&\nu&0&0&0\\ \nu&1&0&0&0\\ 0&0&(1-\nu)/2&0&0\\ 0&0&0&(1-\nu)/2&0\\ 0&0&0&0&(1-\nu)/2\end{pmatrix}\begin{Bmatrix}\varepsilon_x\\ \varepsilon_y\\ \gamma_{xy}\\ \gamma_{yz}\\ \gamma_{xz}\end{Bmatrix} \tag{14}$$

Five governing equations based on five-unknown plate theory employing Hamilton's rule may be introduced as

$$\frac{\partial N_x}{\partial x}+\frac{\partial N_{xy}}{\partial y}=0 \tag{15}$$

$$\frac{\partial N_{xy}}{\partial x}+\frac{\partial N_y}{\partial y}=0 \tag{16}$$

$$\begin{gathered}\frac{\partial^2 M_x}{\partial x^2}+2\frac{\partial^2 M_{xy}}{\partial x\partial y}+\frac{\partial^2 M_y}{\partial y^2}+N_x\frac{\partial^2 w}{\partial x^2}+2N_{xy}\frac{\partial^2 w}{\partial x\partial y}\\ +N_y\frac{\partial^2 w}{\partial y^2}-k_w w+k_P\left(\frac{\partial^2 w}{\partial x^2}+\frac{\partial^2 w}{\partial y^2}\right)=0\end{gathered} \tag{17}$$

$$\frac{\partial S_x}{\partial x}+\frac{\partial S_{xy}}{\partial y}-Q_x=0 \tag{18}$$

$$\frac{\partial S_{xy}}{\partial x}+\frac{\partial S_y}{\partial y}-Q_y=0 \tag{19}$$

in which k_W and k_p are linear and shear foundation parameters and plate forces and moments have been introduced as below relations

$$\begin{gathered}(N_i,M_i,S_i)=\int_{-h/2}^{h/2}(1,z-z^*,\Phi(z)-z^{**})\sigma_i\,dz,\ i=(x,y,xy)\\ Q_i=\int_{-h/2}^{h/2}\Phi'(z)\sigma_j dz,\ j=(xz,yz)\end{gathered} \tag{20}$$

Next, placing Eq. (14) into Eq. (20) results in below relations

$$\begin{gathered}\{N_x,M_x,S_x\}=\frac{1}{1-\nu^2}[\{A_1,A_2,A_3\}\\ (\varepsilon_x^0+\nu\varepsilon_y^0)+\{A_2,A_4,A_5\}(k_x+\nu k_y)\\ +\{A_3,A_5,A_7\}(\chi_x+\nu\chi_y)]\end{gathered} \tag{21}$$

$$\begin{gathered}\{N_y,M_y,S_y\}=\frac{1}{1-\nu^2}[\{A_1,A_2,A_3\}\\ (\varepsilon_y^0+\nu\varepsilon_x^0)+\{A_2,A_4,A_5\}(k_y+\nu k_x)\\ +\{A_3,A_5,A_7\}(\chi_y+\nu\chi_x)]\end{gathered} \tag{22}$$

$$\begin{gathered}\{N_{xy},M_{xy},S_{xy}\}=\frac{1}{2(1+\nu)}\\ [\{A_1,A_2,A_3\}\gamma_{xy}^0+\{A_2,A_4,A_5\}k_{xy}\\ +\{A_3,A_5,A_7\}\chi_{xy}]\end{gathered} \tag{23}$$

$$\{Q_x,Q_y\}=\frac{1}{2(1+\nu)}A_8\{\gamma_{xz}^0,\gamma_{yz}^0\} \tag{24}$$

in which:

$$A_2=0,\ A_1=\int_{-h/2}^{h/2}E(z)\,dz,\ A_3=\int_{-h/2}^{h/2}(\Phi(z)-z^{**})E(z)\,dz,$$
$$A_4=\int_{-h/2}^{h/2}E(z)(z-z^{*})^2\,dz,\ A_5=\int_{-h/2}^{h/2}E(z)(z-z^{*})(\Phi(z)-z^{**})\,dz \quad (25)$$
$$A_7=\int_{-h/2}^{h/2}(\Phi(z)-z^{**})^2E(z)\,dz,\ A_8=\int_{-h/2}^{h/2}(\Phi'(z)-z^{**})^2E(z)\,dz,$$

Next, Eqs. (17)-(19) may be re-written as one equation via placing Eqs. (21)-(24) in Eqs. (17)-(19) and then removing $\psi_{x,x}+\psi_{y,y}$ from derived equations and then adding geometric imperfection effect as

$$\frac{\partial N_x}{\partial x}+\frac{\partial N_{xy}}{\partial y}=0 \quad (26)$$

$$\frac{\partial N_{xy}}{\partial x}+\frac{\partial N_y}{\partial y}=0 \quad (27)$$

$$\begin{aligned}&\left(\Lambda_1\Lambda_3-\Lambda_2^2\right)\nabla^6 w-\Lambda_1\Lambda_4\nabla^4 w-\Lambda_3\nabla^2\\ &(\frac{\partial^2F}{\partial y^2}(\frac{\partial^2w}{\partial x^2}+\frac{\partial^2w^*}{\partial x^2})-2\frac{\partial^2F}{\partial x\partial y}(\frac{\partial^2w}{\partial x\partial y}+\frac{\partial^2w^*}{\partial x\partial y})\\ &+\frac{\partial^2F}{\partial x^2}(\frac{\partial^2w}{\partial y^2}+\frac{\partial^2w^*}{\partial y^2})-k_w w+k_P(\frac{\partial^2w}{\partial x^2}+\frac{\partial^2w}{\partial y^2}))\\ &+\Lambda_4(\frac{\partial^2F}{\partial y^2}(\frac{\partial^2w}{\partial x^2}+\frac{\partial^2w^*}{\partial x^2})\\ &-2\frac{\partial^2F}{\partial x\partial y}(\frac{\partial^2w}{\partial x\partial y}+\frac{\partial^2w^*}{\partial x\partial y})+\frac{\partial^2F}{\partial x^2}(\frac{\partial^2w}{\partial y^2}+\frac{\partial^2w^*}{\partial y^2})\\ &-k_w w+k_P(\frac{\partial^2w}{\partial x^2}+\frac{\partial^2w}{\partial y^2}))=0\end{aligned} \quad (28)$$

in which

$$\begin{aligned}&\Lambda_1=\frac{A_4}{1-\nu^2},\ \Lambda_2=\frac{A_5}{1-\nu^2},\\ &\Lambda_3=\frac{A_1A_7-A_3^2}{A_1(1-\nu^2)},\ \Lambda_4=\frac{A_8}{2(1+\nu)}\end{aligned} \quad (29)$$

and F defines the Airy stress function as

$$\frac{\partial^2F}{\partial y^2}=N_x,\ \frac{\partial^2F}{\partial x\partial y}=-N_{xy},\ \frac{\partial^2F}{\partial x^2}=N_y \quad (30)$$

Moreover, w^* introduces the initial deflection of the plate because of geometric imperfectness. The basic compatibility equation of plates incorporating geometric imperfectness may be written as

$$\begin{aligned}&\frac{\partial^2\varepsilon_x^0}{\partial y^2}+\frac{\partial^2\varepsilon_y^0}{\partial x^2}-\frac{\partial^2\gamma_{xy}^0}{\partial x\partial y}=\left(\frac{\partial^2w}{\partial x\partial y}\right)^2-\frac{\partial^2w}{\partial x^2}\frac{\partial^2w}{\partial y^2}\\ &+2\frac{\partial^2w}{\partial x\partial y}\frac{\partial^2w^*}{\partial x\partial y}-\frac{\partial^2w}{\partial x^2}\frac{\partial^2w^*}{\partial y^2}-\frac{\partial^2w}{\partial y^2}\frac{\partial^2w^*}{\partial x^2}\end{aligned} \quad (31)$$

Next, based on Eqs. (21) and (22), one can derives membrane strains in below forms

$$\begin{aligned}&\varepsilon_x^0=\frac{1}{A_1}[\frac{\partial^2F}{\partial y^2}-\nu\frac{\partial^2F}{\partial x^2}-A_3\chi_x]\\ &\varepsilon_y^0=\frac{1}{A_1}[\frac{\partial^2F}{\partial x^2}-\nu\frac{\partial^2F}{\partial y^2}-A_3\chi_y]\\ &\gamma_{xy}^0=-\frac{1}{A_1}[2(1+\nu)\frac{\partial^2F}{\partial x\partial y}+A_3\chi_{xy}]\end{aligned} \quad (32)$$

Finally, the compatibility equation may be written via below relation via placing Eq. (32) in Eq. (31)

$$\begin{aligned}&\nabla^4F-A_1\left[\left(\frac{\partial^2w}{\partial x\partial y}\right)^2-\frac{\partial^2w}{\partial x^2}\frac{\partial^2w}{\partial y^2}\right.\\ &\left.+2\frac{\partial^2w}{\partial x\partial y}\frac{\partial^2w^*}{\partial x\partial y}-\frac{\partial^2w}{\partial x^2}\frac{\partial^2w^*}{\partial y^2}-\frac{\partial^2w}{\partial y^2}\frac{\partial^2w^*}{\partial x^2}\right]=0\end{aligned} \quad (33)$$

This equation should be simultaneously solved with Eq. (28) for deriving post-buckling path of GOP-reinforced plates.

4. Method of solution

Presented in this chapter is analytic solution of the non-linear governing equations for post-buckling of a GOP-reinforced plate. The below movable edge conditions may be introduced for mechanical post-buckling analyzes of simply-supported plate as:

$$w=N_{xy}=M_x=\frac{\partial^2F}{\partial x\partial y}=0,\ \int_0^b\frac{\partial^2F}{\partial y^2}dy=-P_xbh \quad \text{at } x=0,a \quad (34)$$

$$w=N_{xy}=M_y=\frac{\partial^2F}{\partial x\partial y}=0,\ \int_0^a\frac{\partial^2F}{\partial x^2}dy=-P_yah \quad \text{at } y=0,b \quad (35)$$

Then, the deflections have been selected as below forms

$$w=\sum_{m=1}^{\infty}\sum_{n=1}^{\infty}\tilde{W}\sin(\lambda_m x)\sin(\delta_n y) \quad (36)$$

$$w^*=\sum_{m=1}^{\infty}\sum_{n=1}^{\infty}W^*\sin(\lambda_m x)\sin(\delta_n y) \quad (37)$$

so that $\tilde{W}$ and W^* define plate center deflection and imperfectness magnitude, respectively and $\lambda_m=m\pi/a$, $\delta_n=n\pi/b$. Via utilizing the edge conditions in Eqs.(34)-(35) and displacements in Eqs. (36)-(37), the closed form of stress function F may be defined by

$$\begin{aligned}&F=\Gamma_1\cos(2\lambda_m x)+\Gamma_2\cos(2\delta_n y)\\ &+\Gamma_3\sin(\lambda_m x)\sin(\delta_n y)+\frac{1}{2}P_x y^2+\frac{1}{2}P_y x^2\end{aligned} \quad (38)$$

where

$$\Gamma_1=\frac{A_1\delta_n^2}{32\lambda_m^2}\tilde{W}(\tilde{W}+2W^*),\ \Gamma_1=\frac{A_1\lambda_m^2}{32\delta_n^2}\tilde{W}(\tilde{W}+2W^*),\ \Gamma_3=0$$

Now, Eqs. (36)-(38) can be inserted in Eq. (28) to find the governing equation as

$$\begin{aligned}&K_s\tilde{W}+G_1\tilde{W}^3+G_2\tilde{W}^2W^*\\ &+G_3\tilde{W}\left(W^*\right)^2+\Psi_sW^*=0\end{aligned} \quad (39)$$

where K_s and Ψ_s are the linear stiffness matrices of perfect and imperfect plates respectively. G_i denote nonlinear stiffness matrices. In this study, the biaxial load has been assumed as $P_x=P_y=P$. The nonlinear governing equation has been solved for finding post-buckling curves of the plate based on the variation of P versus normalized deflection $\tilde{W}/h$. It must be pointed out that calculations have been carried out based on the below normalized quantities for

Table 1 Comparison of post-buckling loads of ideal and imperfect plates for various normalized amplitude

$\bar{W}/h$	w^*/h=0		w^*/h=0.1	
	Chikh *et al*. (2016)	present	Chikh *et al*. (2016)	present
0	0.62411	0.62411	0	0
0.1	0.62627	0.62627	0.31853	0.31853
0.2	0.63274	0.63274	0.43334	0.43334
0.3	0.64354	0.64354	0.50047	0.50047

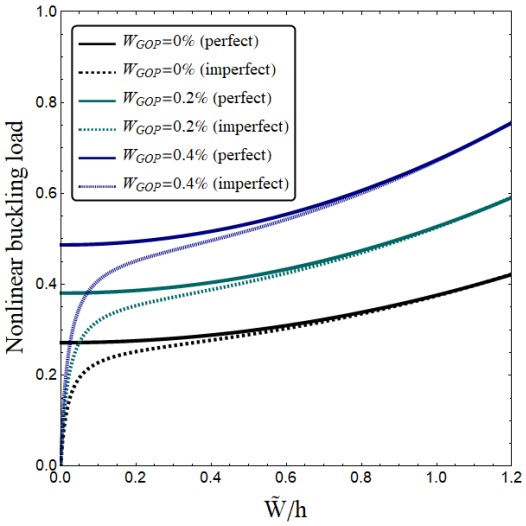

Fig. 2 Post-buckling load of GOP-reinforced plate versus dimensionless deflection for different GOP weight fractions (a/h=10, K_W=K_P=0, W^*/h=0.02)

elastic foundation

$$K_W = \mathrm{k}_W \frac{\mathrm{a}^4}{D},\ K_p = \mathrm{k}_p \frac{\mathrm{a}^2}{D} \tag{40}$$

5. Discussion on results

In this section, post-buckling of a GOP-reinforced plate modeled via nonlinear five-unknown plate theory has been studied based upon provided solution approach. The dependency of post-buckling load on GOPs, foundation parameters, normalized amplitude, matrix material, geometric imperfectness and shear deformation will be explored. As the first step, post-buckling responses of ideal and imperfect plates have been validated with those reported by Chikh *et al*. (2016) based on functionally graded (FG) plate model, as provided in Table 1. According to the table, buckling loads have been provided for both perfect (w^*/h=0) and imperfect (w^*/h=0.1) plates based on various normalized amplitude. In this research, the material properties of GOP reinforced beam with concrete matrix have been considered as:

- $E_{GOP} = 444.8\ GPa$, $d_{GOP} = 500\ nm$, $t_{GOP} = 0.95\ nm$, $v_{GOP} = 0.165$.
- $E_M = 16.9\ GPa$, $v_M = 0.15$.

Influences of GOP weight fraction on the post-buckling properties of concrete plates are presented in Fig. 2 at imperfection amplitude of W^*/h=0.02. Uniform GOP distribution has been considered. In the case of ideal (perfect) GOP-reinforced plate, the load at $\bar{W}/h = 0$ is critical buckling load. However, in the case of imperfect GOP-reinforced plate ($w^*/h\neq0$), the critical buckling load does not exist, because the plate has an initial deflection. It must be pointed out that the buckling load becomes greater by increasing in normalized amplitude. The reason is intrinsic stiffening impact raised from geometric nonlinearity. Reinforcing effect of GOPs on mechanical properties of the plate is obviously observable from this graph. In fact, the effective stiffness of the reinforced concrete plate may be prominently strengthened via adding a small amount of GOPs to matrix material (concrete). Thus, post-buckling loads enlarge by increasing in GOP weight fraction (W_{GOP}).

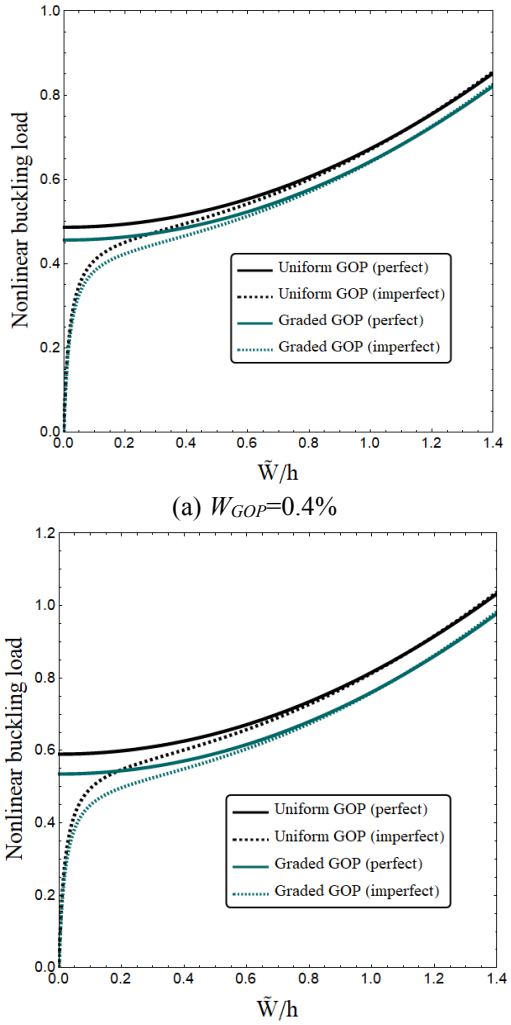

(a) W_{GOP}=0.4%

(b) W_{GOP}=0.6%

Fig. 3 Post-buckling load of GOP-reinforced plate versus dimensionless deflection for different GOP distributions (a/h=10, K_W=K_P, W^*/h=0.02)

In Fig. 3, post-buckling load-amplitude curves of a GOP-reinforced concrete plate with and without geometric imperfections have been presented accounting for various GOP weight fraction and dispersions. It is considered that a/h=10 and W^*=0.02h. The most important observation from this figure is that increasing GOP weight fraction

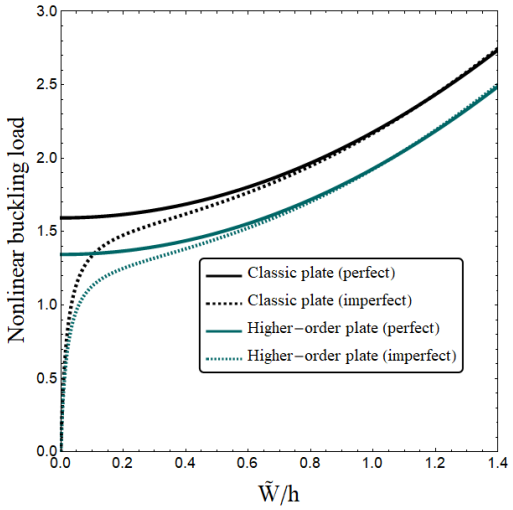

Fig. 4 Post-buckling load of GOP-reinforced plate versus dimensionless deflection for different plate theories (a/h=5, K_W=K_P=0, W_{GOP}=0.2%, W^*/h=0.02)

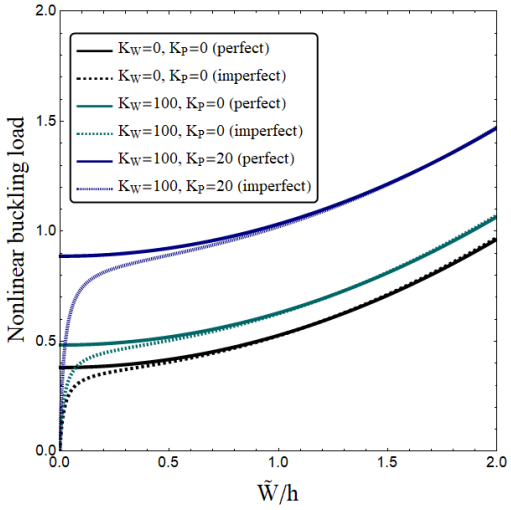

Fig. 6 Post-buckling load of GOP-reinforced plate versus dimensionless deflection for different foundation parameters (a/h=10, W_{GOP}=0.2 %)

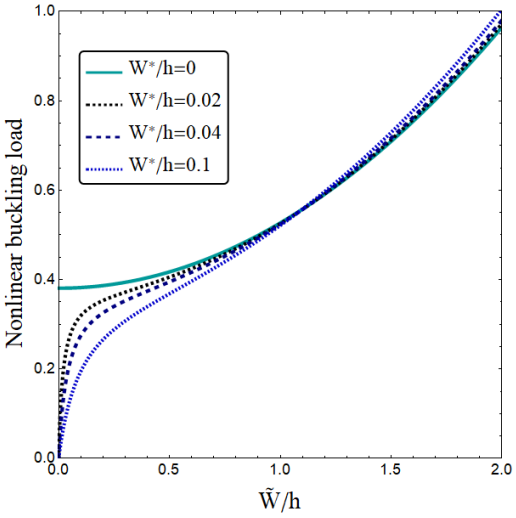

Fig. 5 Post-buckling load of GOP-reinforced plate versus dimensionless deflection for different geometric imperfections (a/h=10, K_W=K_P= 0, W_{GOP}=0.2%)

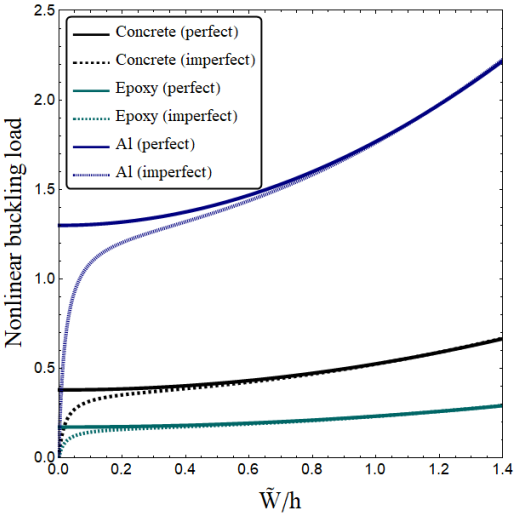

Fig. 7 Post-buckling load of GOP-reinforced plate versus dimensionless deflection for matrix materials (a/h=10, W_{GOP}=0.2 %)

yields larger buckling loads for all types of GOP distributions. It means that adding the amount of GOP can increase the plate stiffness and enhance its post-buckling behavior. Moreover, uniform GOP distribution provides greater post-buckling loads than linear (graded) distribution. This is due to larger amount of GOP at the upper surface of nano-composite plate. As an outcome, controlling of GOP is vital for obtaining the best mechanical performances of concrete plates.

Shear deformation effect on post-buckling behavior of concrete GOP-reinforced plate has been plotted in Fig. 4 via comparison of obtained results for classic and higher-order plate models. Geometric imperfection amplitude is selected as W^*/h=0.02. This figure shows that higher-order plate model gives lower post-buckling loads than classic plate theory due to incorporating shear deformation effect. So, the presented higher-order plate formulation is more accurate for post-buckling analysis of thick concrete GOP-reinforced plates.

Geometrical imperfection (W^*/h) effect on post-buckling behavior of concrete GOP-reinforced plate has been illustrated in Fig. 5. IT may be observed that the initial deflection of plate has notable influences on the post-buckling load-deflection path. Based on previous discussion, the critical buckling load vanishes by considering plate initial deflection. In fact, for the case of perfect structure (w^*/h=0), the plate has critical buckling. Next, plate buckling capacity improves by the increase of normalized deflection. However, for the case of imperfect structure ($w^*/h\neq0$), there is no buckling load before the initial situation of GOP-reinforced plate. Thus, the buckling load is zero at the starting point for imperfect plates. After that, greater amplitudes of plates need stronger compressive load. Finally, it may be concluded that pot-buckling curves of perfect and imperfect plates become closer to each other at large values for normalized amplitude.

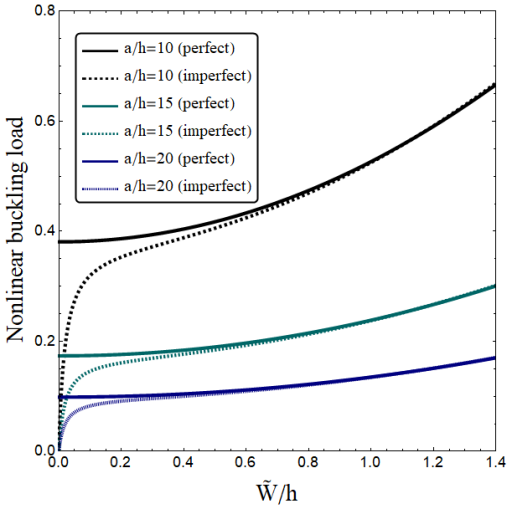

Fig. 8 Post-buckling load of GOP-reinforced plate versus dimensionless deflection for different length to thickness ratios (W_{GOP}=0.2 %)

Fig. 6 indicates the variation of post-buckling load of a GOP-reinforced plate versus normalized amplitude for various linear (K_W), shear (K_P) foundation factors at W_{GOP}=0.2%. It must be pointed out that the shear layer gives continuous interactions with the GOP-reinforced plate, whereas linear layer gives discontinuous interactions with the plate. Growth of foundation factors results in greater nonlinear buckling load via improving the bending rigidity of GOP-reinforced plate.

Fig. 7 illustrates the effect of matrix material on post-buckling curves of the plate at a prescribed amount of GOPs (W_{GOP}=0.2 %). Three types of material including concrete, epoxy (E=3.5 GPa) and Aluminum (E=70 GPa) are considered as matrix material. The maximum and minimum values of buckling loads are obtained for Aluminum and epoxy matrices. Actually, epoxy matrix gives smaller post-buckling loads than concrete matrix due to having lower stiffness. Accordingly, type of matrix material has a key role on post-buckling behavior of ideal/imperfect GOP-reinforced plates.

Effects of length-to-thickness ratio (a/h) on post-buckling behaviors of GOP-reinforced plates have been plotted in Fig. 8. Two cases of geometrically ideal (perfect) and imperfect plates have been supposed. It is obvious that plates are less rigid at greater values for a/h. Accordingly, derived post-buckling load becomes lower via enlargement of a/h at prescribed normalized amplitudes ($\widetilde{W}/h$). Also, calculated post-buckling loads for various values of a/h rely on the magnitude of normalized deflection. For smaller a/h, post-buckling load increases with a higher slope according to normalized deflection than higher length-to-thickness ratio or thinner plates. Such observation is due to more stiffness of the plate at low values of a/h.

6. Conclusions

This article analyzed post-buckling behaviors of imperfect concrete plates filled by GOPs via stablishing a nonlinear higher order plate formulation in which shear deformation effects are involved without adding shear correction factor. Both uniform and linear GOP distributions were considered. Obtained finding in this research are presented as follows.

- The most important observation was that increasing GOP weight fraction yields larger buckling loads for all types of GOP distributions. It means that adding the amount of GOP can increase the plate stiffness and enhance its post-buckling behavior.
- Moreover, uniform GOP distribution provided greater post-buckling loads than linear distribution. This is due to larger amount of GOP at the upper surface of nano-composite plate.
- It was found that refined plate model gives lower post-buckling loads than classic plate theory due to incorporating shear deformation effect.
- An important finding was that as the magnitude of imperfection is greater, the post-buckling load is lower.

References

Abualnour, M., Chikh, A., Hebali, H., Kaci, A., Tounsi, A., Bousahla, A.A. and Tounsi, A. (2019), "Thermomechanical analysis of antisymmetric laminated reinforced composite plates using a new four variable trigonometric refined plate theory", *Comput. Concrete*, **24**(6), 489-498. https://doi.org/10.12989/cac.2019.24.6.489.

Addou, F.Y., Meradjah, M., Bousahla, A.A., Benachour, A., Bourada, F., Tounsi, A. and Mahmoud, S.R. (2019), "Influences of porosity on dynamic response of FG plates resting on Winkler/Pasternak/Kerr foundation using quasi 3D HSDT", *Comput. Concrete*, **24**(4), 347-367. https://doi.org/10.12989/cac.2019.24.4.347.

Ahankari, S.S. and Kar, K.K. (2010), "Hysteresis measurements and dynamic mechanical characterization of functionally graded natural rubber-carbon black composites", *Polym. Eng. Sci.*, **50**(5), 871-877. https://doi.org/10.1002/pen.21601.

Ahmed, R.A., Fenjan, R.M. and Faleh, N.M. (2019), "Analyzing post-buckling behavior of continuously graded FG nanobeams with geometrical imperfections", *Geomech. Eng.*, **17**(2), 175-180. https://doi.org/10.12989/gae.2019.17.2.175.

Al-Maliki, A.F., Faleh, N.M. and Alasadi, A.A. (2019), "Finite element formulation and vibration of nonlocal refined metal foam beams with symmetric and non-symmetric porosities", *Struct. Monit. Mainten.*, **6**(2), 147-159. https://doi.org/10.12989/smm.2019.6.2.147.

Alijani, M. and Bidgoli, M.R. (2018), "Agglomerated SiO_2 nanoparticles reinforced-concrete foundations based on higher order shear deformation theory: Vibration analysis", *Adv. Concrete Constr.*, **6**(6), 585. https://doi.org/10.12989/acc.2018.6.6.585.

Alimirzaei, S., Mohammadimehr, M. and Tounsi, A. (2019), "Nonlinear analysis of viscoelastic micro-composite beam with geometrical imperfection using FEM: MSGT electro-magneto-elastic bending, buckling and vibration solutions", *Struct. Eng. Mech.*, **71**(5), 485-502. https://doi.org/10.12989/sem.2019.71.5.485.

Azimi, M., Mirjavadi, S.S., Shafiei, N. and Hamouda, A.M.S. (2017), "Thermo-mechanical vibration of rotating axially functionally graded nonlocal Timoshenko beam", *Appl. Phys. A*, **123**(1), 104. http://dx.doi.org/10.1007/s00339-017-0772-1.

Azimi, M., Mirjavadi, S.S., Shafiei, N., Hamouda, A.M.S. and Davari, E. (2018), "Vibration of rotating functionally graded

Timoshenko nano-beams with nonlinear thermal distribution", *Mech. Adv. Mater. Struct.*, **25**(6), 467-480. https://doi.org/10.1080/15376494.2017.1285455.

Balubaid, M., Tounsi, A., Dakhel, B. and Mahmoud, S.R. (2019), "Free vibration investigation of FG nanoscale plate using nonlocal two variables integral refined plate theory", *Comput. Concrete*, **24**(6), 579-586. https://doi.org/10.12989/cac.2019.24.6.579.

Barati, M.R. (2017), "Nonlocal-strain gradient forced vibration analysis of metal foam nanoplates with uniform and graded porosities", *Adv. Nano Res.*, **5**(4), 393-414. https://doi.org/10.12989/anr.2017.5.4.393.

Barati, M.R. and Zenkour, A.M. (2018), "Analysis of postbuckling of graded porous GPL-reinforced beams with geometrical imperfection", *Mech. Adv. Mater. Struct.*, **26**(6), 503-511. https://doi.org/10.1080/15376494.2017.1400622.

Batou, B., Nebab, M., Bennai, R., Atmane, H.A., Tounsi, A. and Bouremana, M. (2019), "Wave dispersion properties in imperfect sigmoid plates using various HSDTs", *Steel Compos. Struct.*, **33**(5), 699-716. https://doi.org/10.12989/scs.2019.33.5.699.

Bedia, W.A., Houari, M.S.A., Bessaim, A., Bousahla, A.A., Tounsi, A., Saeed, T. and Alhodaly, M.S. (2019), "A new hyperbolic two-unknown beam model for bending and buckling analysis of a nonlocal strain gradient nanobeams", *J. Nano Res.*, **57**, 175-191. https://doi.org/10.4028/www.scientific.net/JNanoR.57.175.

Belbachir, N., Draich, K., Bousahla, A.A., Bourada, M., Tounsi, A. and Mohammadimehr, M. (2019), "Bending analysis of anti-symmetric cross-ply laminated plates under nonlinear thermal and mechanical loadings", *Steel Compos. Struct.*, **33**(1), 913-924. https://doi.org/10.12989/scs.2019.33.1.081.

Berghouti, H., Adda Bedia, E.A., Benkhedda, A. and Tounsi, A. (2019), "Vibration analysis of nonlocal porous nanobeams made of functionally graded material", *Adv. Nano Res.*, **7**(5), 351-364. https://doi.org/10.12989/anr.2019.7.5.351.

Boukhlif, Z., Bouremana, M., Bourada, F., Bousahla, A.A., Bourada, M., Tounsi, A. and Al-Osta, M.A. (2019), "A simple quasi-3D HSDT for the dynamics analysis of FG thick plate on elastic foundation", *Steel Compos. Struct.*, **31**(5), 503-516. https://doi.org/10.12989/scs.2019.31.5.503.

Boulefrakh, L., Hebali, H., Chikh, A., Bousahla, A.A., Tounsi, A. and Mahmoud, S.R. (2019), "The effect of parameters of visco-Pasternak foundation on the bending and vibration properties of a thick FG plate", *Geomech. Eng.*, **18**(2), 161-178. https://doi.org/10.12989/gae.2019.18.2.161.

Bounouara, F., Benrahou, K.H., Belkorissat, I. and Tounsi, A. (2016), "A nonlocal zeroth-order shear deformation theory for free vibration of functionally graded nanoscale plates resting on elastic foundation", *Steel Compos. Struct.*, **20**(2), 227-249. https://doi.org/10.12989/scs.2016.20.2.227.

Bourada, F., Bousahla, A.A., Bourada, M., Azzaz, A., Zinata, A. and Tounsi, A. (2019), "Dynamic investigation of porous functionally graded beam using a sinusoidal shear deformation theory", *Wind Struct.*, **28**(1), 19-30. https://doi.org/10.12989/was.2019.28.1.019.

Boutaleb, S., Benrahou, K.H., Bakora, A., Algarni, A., Bousahla, A.A., Tounsi, A., ... & Mahmoud, S.R. (2019), "Dynamic analysis of nanosize FG rectangular plates based on simple nonlocal quasi 3D HSDT", *Adv. Nano Res.*, **7**(3), 189-206. https://doi.org/10.12989/anr.2019.7.3.191.

Chaabane, L. A., Bourada, F., Sekkal, M., Zerouati, S., Zaoui, F.Z., Tounsi, A., ... & Tounsi, A. (2019), "Analytical study of bending and free vibration responses of functionally graded beams resting on elastic foundation", *Struct. Eng. Mech.*, **71**(2), 185-196. https://doi.org/10.12989/sem.2019.71.2.185.

Chikh, A., Bakora, A., Heireche, H., Houari, M.S.A., Tounsi, A. and Bedia, E.A. (2016), "Thermo-mechanical postbuckling of symmetric S-FGM plates resting on Pasternak elastic foundations using hyperbolic shear deformation theory", *Struct. Eng. Mech.*, **57**(4), 617-639. https://doi.org/10.12989/sem.2016.57.4.617.

Dehrouyeh-Semnani, A.M. (2018), "On the thermally induced non-linear response of functionally graded beams", *Int. J. Eng. Sci.*, **125**, 53-74. https://doi.org/10.1016/j.ijengsci.2017.12.001.

Dehrouyeh-Semnani, A.M. and Jafarpour, S. (2019), "Nonlinear thermal stability of temperature-dependent metal matrix composite shallow arches with functionally graded fiber reinforcements", *Int. J. Mech. Sci.*, **161**, 105075.

Dehrouyeh-Semnani, A.M., Dehdashti, E., Yazdi, M.R.H. and Nikkhah-Bahrami, M. (2019), "Nonlinear thermo-resonant behavior of fluid-conveying FG pipes", *Int. J. Eng. Sci.*, **144**, 103141. https://doi.org/10.1016/j.ijengsci.2019.103141.

Draiche, K., Bousahla, A.A., Tounsi, A., Alwabli, A.S., Tounsi, A. and Mahmoud, S.R. (2019), "Static analysis of laminated reinforced composite plates using a simple first-order shear deformation theory", *Comput. Concrete*, **24**(4), 369-378. https://doi.org/10.12989/cac.2019.24.4.369.

Draoui, A., Zidour, M., Tounsi, A. and Adim, B. (2019), "Static and dynamic behavior of nanotubes-reinforced sandwich plates using (FSDT)", *J. Nano Res.*, **57**, 117-135. https://doi.org/10.4028/www.scientific.net/JNanoR.57.117.

Du, H., Gao, H.J. and Dai Pang, S. (2016), "Improvement in concrete resistance against water and chloride ingress by adding graphene nanoplatelet", *Cement Concrete Res.*, **83**, 114-123. https://doi.org/10.1016/j.cemconres.2016.02.005.

Esawi, A.M.K., Morsi, K., Sayed, A., Taher, M. and Lanka, S. (2011), "The influence of carbon nanotube (CNT) morphology and diameter on the processing and properties of CNT-reinforced aluminium composites", *Compos. Part A: Appl. Sci. Manuf.*, **42**(3), 234-243. https://doi.org/10.1016/j.compositesa.2010.11.008.

Faleh, N.M., Ahmed, R.A. and Fenjan, R.M. (2018), "On vibrations of porous FG nanoshells", *Int. J. Eng. Sci.*, **133**, 1-14. https://doi.org/10.1016/j.ijengsci.2018.08.007.

Fang, M., Wang, K., Lu, H., Yang, Y. and Nutt, S. (2009). Covalent polymer functionalization of graphene nanosheets and mechanical properties of composites", *J. Mater. Chem.*, **19**(38), 7098-7105. https://doi.org/10.1039/B908220D.

Feng, C., Kitipornchai, S. and Yang, J. (2017), "Nonlinear free vibration of functionally graded polymer composite beams reinforced with graphene nanoplatelets (GPLs)", *Eng. Struct.*, **140**, 110-119. https://doi.org/10.1016/j.engstruct.2017.02.052.

Fenjan, R.M., Ahmed, R.A., Alasadi, A.A. and Faleh, N.M. (2019), "Nonlocal strain gradient thermal vibration analysis of double-coupled metal foam plate system with uniform and non-uniform porosities", *Coupl. Syst. Mech.*, **8**(3), 247-257. https://doi.org/10.12989/csm.2019.8.3.247.

Gojny, F.H., Wichmann, M.H.G., Köpke, U., Fiedler, B. and Schulte, K. (2004), "Carbon nanotube-reinforced epoxy-composites: enhanced stiffness and fracture toughness at low nanotube content", *Compos. Sci. Technol.*, **64**(15), 2363-2371. https://doi.org/10.1016/j.compscitech.2004.04.002.

Guenaneche, B., Benyoucef, S., Tounsi, A. and Adda Bedia, E.A. (2019), "Improved analytical method for adhesive stresses in plated beam: Effect of shear deformation", *Adv. Concrete Constr.*, **7**(3), 151-166. https://doi.org/10.12989/acc.2019.7.3.151.

Hellal, H., Bourada, M., Hebali, H., Bourada, F., Tounsi, A., Bousahla, A.A. and Mahmoud, S.R. (2019), "Dynamic and stability analysis of functionally graded material sandwich plates in hygro-thermal environment using a simple higher shear deformation theory", *J. Sandw. Struct. Mater.*, 1099636219845841. https://doi.org/10.1177/1099636219845841.

Hussain, M., Naeem, M.N., Tounsi, A. and Taj, M. (2019),

"Nonlocal effect on the vibration of armchair and zigzag SWCNTs with bending rigidity", *Adv. Nano Res.*, **7**(6), 431-442. https://doi.org/10.12989/anr.2019.7.6.431.

Kaddari, M., Kaci, A., Bousahla, A.A., Tounsi, A., Bourada, F., Bedia, E.A. and Al-Osta, M.A. (2020), "A study on the structural behaviour of functionally graded porous plates on elastic foundation using a new quasi-3D model: Bending and Free vibration analysis", *Comput. Concrete*, **25**(1), 37-57. https://doi.org/10.12989/cac.2020.25.1.037.

Keleshteri, M.M., Asadi, H. and Wang, Q. (2017), "Large amplitude vibration of FG-CNT reinforced composite annular plates with integrated piezoelectric layers on elastic foundation", *Thin Wall. Struct.*, **120**, 203-214. https://doi.org/10.1016/j.tws.2017.08.035.

Khiloun, M., Bousahla, A.A., Kaci, A., Bessaim, A., Tounsi, A. and Mahmoud, S.R. (2019), "Analytical modeling of bending and vibration of thick advanced composite plates using a four-variable quasi 3D HSDT", *Eng. Comput.*, 1-15. https://doi.org/10.1007/s00366-019-00732-1.

King, J.A., Klimek, D.R., Miskioglu, I. and Odegard, G.M. (2013), "Mechanical properties of graphene nanoplatelet/epoxy composites", *J. Appl. Polym. Sci.*, **128**(6), 4217-4223. https://doi.org/10.1002/app.38645.

Kitipornchai, S., Chen, D. and Yang, J. (2017). Free vibration and elastic buckling of functionally graded porous beams reinforced by graphene platelets", *Mater. Des.*, **116**, 656-665. https://doi.org/10.1016/j.matdes.2016.12.061.

Lal, A. and Markad, K. (2018), "Deflection and stress behaviour of multi-walled carbon nanotube reinforced laminated composite beams", *Comput. Concrete*, **22**(6), 501-514. https://doi.org/10.12989/cac.2018.22.6.501.

Liew, K.M., Lei, Z.X. and Zhang, L.W. (2015), "Mechanical analysis of functionally graded carbon nanotube reinforced composites: a review", *Compos. Struct.*, **120**, 90-97. https://doi.org/10.1016/j.compstruct.2014.09.041.

Lin, F., Yang, C., Zeng, Q.H. and Xiang, Y. (2018), "Morphological and mechanical properties of graphene-reinforced PMMA nanocomposites using a multiscale analysis", *Comput. Mater. Sci.*, **150**, 107-120. https://doi.org/10.1016/j.commatsci.2018.03.048.

Mahmoudi, A., Benyoucef, S., Tounsi, A., Benachour, A., Adda Bedia, E.A. and Mahmoud, S.R. (2019), "A refined quasi-3D shear deformation theory for thermo-mechanical behavior of functionally graded sandwich plates on elastic foundations", *J. Sandw. Struct. Mater.*, **21**(6), 1906-1926. https://doi.org/10.1177/1099636217727577.

Mahmoudi, A., Benyoucef, S., Tounsi, A., Benachour, A., Adda Bedia, E.A. and Mahmoud, S.R. (2019), "Static and dynamic behavior of (FG-CNT) reinforced porous sandwich plate", *Steel Compos. Struct.*, **32**(5), 595-610. https://doi.org/10.12989/scs.2019.32.5.595.

Meksi, R., Benyoucef, S., Mahmoudi, A., Tounsi, A., Adda Bedia, E.A. and Mahmoud, S.R. (2019), "An analytical solution for bending, buckling and vibration responses of FGM sandwich plates", *J. Sandw. Struct. Mater.*, **21**(2), 727-757. https://doi.org/10.1177/1099636217698443.

Metwally, I.M. (2014), "Three-dimensional finite element analysis of reinforced concrete slabs strengthened with epoxy-bonded steel plates", *Adv. Concrete Constr.*, **2**(2), 91. https://doi.org/10.12989/acc.2014.2.2.091.

Mirjavadi, S.S., Afshari, B.M., Barati, M.R. and Hamouda, A.M.S. (2018), "Strain gradient based dynamic response analysis of heterogeneous cylindrical microshells with porosities under a moving load", *Mater. Res. Exp.*, **6**(3), 035029.

Mirjavadi, S.S., Afshari, B.M., Barati, M.R. and Hamouda, A.M.S. (2019), "Transient response of porous FG nanoplates subjected to various pulse loads based on nonlocal stress-strain gradient theory", *Eur. J. Mech.-A/Solid.*, **74**, 210-220. https://doi.org/10.1016/j.euromechsol.2018.11.004.

Mirjavadi, S.S., Afshari, B.M., Barati, M.R. and Hamouda, A.M.S. (2019), "Nonlinear free and forced vibrations of graphene nanoplatelet reinforced microbeams with geometrical imperfection", *Microsyst. Technol.*, **25**, 3137-3150. https://doi.org/10.1007/s00542-018-4277-4.

Mirjavadi, S.S., Afshari, B.M., Khezel, M., Shafiei, N., Rabby, S. and Kordnejad, M. (2018), "Nonlinear vibration and buckling of functionally graded porous nanoscaled beams", *J. Brazil. Soc. Mech. Sci. Eng.*, **40**(7), 352. https://doi.org/10.1007/s40430-018-1272-8.

Mirjavadi, S.S., Afshari, B.M., Shafiei, N., Hamouda, A.M.S. and Kazemi, M. (2017), "Thermal vibration of two-dimensional functionally graded (2D-FG) porous Timoshenko nanobeams", *Steel Compos. Struct.*, **25**(4), 415-426. https://doi.org/10.12989/scs.2017.25.4.415.

Mirjavadi, S.S., Forsat, M., Barati, M.R., Abdella, G.M., Afshari, B.M., Hamouda, A.M.S. and Rabby, S. (2019), "Dynamic response of metal foam FG porous cylindrical micro-shells due to moving loads with strain gradient size-dependency", *Eur. Phys. J. Plus*, **134**(5), 214. https://doi.org/10.1140/epjp/i2019-12540-3.

Mirjavadi, S.S., Forsat, M., Barati, M.R., Abdella, G.M., Hamouda, A.M.S., Afshari, B.M. and Rabby, S. (2019), "Post-buckling analysis of piezo-magnetic nanobeams with geometrical imperfection and different piezoelectric contents", *Microsyst. Technol.*, **25**(9), 3477-3488. https://doi.org/10.1007/s00542-018-4241-3.

Mirjavadi, S.S., Forsat, M., Hamouda, A.M.S. and Barati, M.R. (2019), "Dynamic response of functionally graded graphene nanoplatelet reinforced shells with porosity distributions under transverse dynamic loads", *Mater. Res. Exp.*, **6**(7), 075045.

Mirjavadi, S.S., Forsat, M., Nikookar, M., Barati, M.R. and Hamouda, A.M.S. (2019), "Nonlinear forced vibrations of sandwich smart nanobeams with two-phase piezo-magnetic face sheets", *Eur. Phys. J. Plus*, **134**(10), 508. https://doi.org/10.1140/epjp/i2019-12806-8.

Mirjavadi, S.S., Rabby, S., Shafiei, N., Afshari, B.M. and Kazemi, M. (2017), "On size-dependent free vibration and thermal buckling of axially functionally graded nanobeams in thermal environment", *Appl. Phys. A*, **123**(5), 315. https://doi.org/10.1007/s00339-017-0918-1.

Mohammed, A., Sanjayan, J.G., Nazari, A. and Al-Saadi, N.T.K. (2017), "Effects of graphene oxide in enhancing the performance of concrete exposed to high-temperature", *Aust. J. Civil Eng.*, **15**(1), 61-71. https://doi.org/10.1080/14488353.2017.1372849.

Mouffoki, A., Bedia, E.A., Houari, M.S.A., Tounsi, A. and Mahmoud, S.R. (2017), "Vibration analysis of nonlocal advanced nanobeams in hygro-thermal environment using a new two-unknown trigonometric shear deformation beam theory", *Smart Struct. Syst.*, **20**(3), 369-383. https://doi.org/10.12989/sss.2017.20.3.369.

Nieto, A., Bisht, A., Lahiri, D., Zhang, C. and Agarwal, A. (2017), "Graphene reinforced metal and ceramic matrix composites: a review", *Int. Mater. Rev.*, **62**(5), 241-302. https://doi.org/10.1080/09506608.2016.1219481.

Rafiee, M.A., Rafiee, J., Wang, Z., Song, H., Yu, Z.Z. and Koratkar, N. (2009), "Enhanced mechanical properties of nanocomposites at low graphene content", *ACS Nano*, **3**(12), 3884-3890. https://doi.org/10.1021/nn9010472.

Rezaiee-Pajand, M., Masoodi, A.R. and Mokhtari, M. (2018), "Static analysis of functionally graded non-prismatic sandwich beams", *Adv. Comput. Des.*, **3**(2), 165-190. https://doi.org/10.12989/acd.2018.3.2.165.

Sahla, M., Saidi, H., Draiche, K., Bousahla, A.A., Bourada, F. and Tounsi, A. (2019), "Free vibration analysis of angle-ply laminated composite and soft core sandwich plates", *Steel Compos. Struct.*, **33**(5), 663-679. https://doi.org/10.12989/scs.2019.33.5.663.

Semmah, A., Heireche, H., Bousahla, A.A. and Tounsi, A. (2019), "Thermal buckling analysis of SWBNNT on Winkler foundation by non local FSDT", *Adv. Nano Res.*, **7**(2), 89-98. https://doi.org/10.12989/anr.2019.7.2.089.

Shafiei, N., Mirjavadi, S.S., Afshari, B.M., Rabby, S. and Hamouda, A.M.S. (2017), "Nonlinear thermal buckling of axially functionally graded micro and nanobeams", *Compos. Struct.*, **168**, 428-439. https://doi.org/10.1016/j.compstruct.2017.02.048.

Shamsaei, E., de Souza, F.B., Yao, X., Benhelal, E., Akbari, A. and Duan, W. (2018), "Graphene-based nanosheets for stronger and more durable concrete: A review", *Constr. Build. Mater.*, **183**, 642-660. https://doi.org/10.1016/j.conbuildmat.2018.06.201.

Shen, H.S., Xiang, Y., Lin, F. and Hui, D. (2017), "Buckling and postbuckling of functionally graded graphene-reinforced composite laminated plates in thermal environments", *Compos. Part B: Eng.*, **119**, 67-78. https://doi.org/10.1016/j.compositesb.2017.03.020.

Song, M., Kitipornchai, S. and Yang, J. (2017), "Free and forced vibrations of functionally graded polymer composite plates reinforced with graphene nanoplatelets", *Compos. Struct.*, **159**, 579-588. https://doi.org/10.1016/j.compstruct.2016.09.070.

Tlidji, Y., Zidour, M., Draiche, K., Safa, A., Bourada, M., Tounsi, A., ... & Mahmoud, S.R. (2019), "Vibration analysis of different material distributions of functionally graded microbeam", *Struct. Eng. Mech.*, **69**(6), 637-649. https://doi.org/10.12989/sem.2019.69.6.637.

Wang, L. and Su, R.K.L. (2013), "A unified design procedure for preloaded rectangular RC columns strengthened with post-compressed plates", *Adv. Concrete Constr.*, **1**(2), 163. https://doi.org/10.12989/acc.2013.1.2.163.

Yang, B., Yang, J. and Kitipornchai, S. (2017), "Thermoelastic analysis of functionally graded graphene reinforced rectangular plates based on 3D elasticity", *Meccanica*, **52**(10), 2275-2292. https://doi.org/10.1007/s11012-016-0579-8.

Zaheer, M.M., Jafri, M.S. and Sharma, R. (2019), "Effect of diameter of MWCNT reinforcements on the mechanical properties of cement composites", *Adv. Concrete Constr.*, **8**(3), 207-215. https://doi.org/10.12989/acc.2019.8.3.207.

Zaoui, F.Z., Ouinas, D. and Tounsi, A. (2019), "New 2D and quasi-3D shear deformation theories for free vibration of functionally graded plates on elastic foundations", *Compos. Part B*, **159**, 231-247. https://doi.org/10.1016/j.compositesb.2018.09.051.

Zarga, D., Tounsi, A., Bousahla, A.A., Bourada, F. and Mahmoud, S.R. (2019), "Thermomechanical bending study for functionally graded sandwich plates using a simple quasi-3D shear deformation theory", *Steel Compos. Struct.*, **32**(3), 389-410. https://doi.org/10.12989/scs.2019.32.3.389.

Zemri, A., Houari, M.S.A., Bousahla, A.A. and Tounsi, A. (2015), "A mechanical response of functionally graded nanoscale beam: an assessment of a refined nonlocal shear deformation theory beam theory", *Struct. Eng. Mech.*, **54**(4), 693-710. https://doi.org/10.12989/sem.2015.54.4.693.

Zhang, L.W. (2017), "On the study of the effect of in-plane forces on the frequency parameters of CNT-reinforced composite skew plates", *Compos. Struct.*, **160**, 824-837. https://doi.org/10.1016/j.compstruct.2016.10.116.

Zhang, Z., Li, Y., Wu, H., Zhang, H., Wu, H., Jiang, S. and Chai, G. (2020), "Mechanical analysis of functionally graded graphene oxide-reinforced composite beams based on the first-order shear deformation theory", *Mech. Adv. Mater. Struct.*, **27**, 3-11. https://doi.org/10.1080/15376494.2018.1444216.

CC